



ELSEVIER

Mathematics and Computers in Simulation 50 (1999) 527–539



MATHEMATICS
AND
COMPUTERS
IN SIMULATION

www.elsevier.nl/locate/matcom

Recovery of surface parameters from stepped-frequency radar returns

Margaret Cheney^{a,*}, David Isaacson^a, Victoria I. Lytle^b, Stephen F. Ackley^c

^a*Department of Mathematical Sciences, Rensselaer Polytechnic Institute, Troy, NY 12180, USA*

^b*Antarctic CRC and Australian Antarctic Division, Hobart, Tasmania 7001, Australia*

^c*USA CRREL, 72 Lyme Rd., Hanover, NH 03755, USA*

Abstract

This paper discusses a method for using the reflected signal from a stepped-frequency radar system to obtain the electrical permittivity and conductivity in a thin layer at the flat surface of a (possibly inhomogeneous) body. The method is based on a band-limited version of geometrical optics. © 1999 IMACS/Elsevier Science B.V. All rights reserved.

Keywords: Inverse problem; Sea ice; Progressing wave expansion

1. Introduction

This work is motivated by the problem of remote sensing of sea ice [1]. There are several reasons for interest in this topic. First, it is hoped that remote electromagnetic measurements will provide information about the electric properties, and then it is hoped that knowledge of the electric properties can eventually be translated into information about the ice's physical properties. Knowledge of these properties would, in turn, be very useful as an aid to ship navigation and other operations in ice-covered regions, such as landing planes on ice. Another reason for interest in sea ice is its importance in global climate models. Because of the remoteness of polar regions, satellite sensors are the only feasible way to routinely monitor these regions on a global scale. Knowledge of the dielectric constant of ice, particularly in the microwave spectrum, is important to the interpretation of remotely sensed data.

Sea ice is a multi-phase medium, which is found at temperatures near its melting point. As salt water freezes, the salt cannot easily be incorporated into the ice crystal matrix, so small pockets of brine tend to form. The size and number of these pockets depends on the temperature of the ice and on its history. As ice ages, these pockets tend to drain, leaving pockets of air in the portion of the ice above sea level. Because brine and air have very different electrical properties from ice, these pockets scatter electromagnetic waves strongly [20].

* Corresponding author.

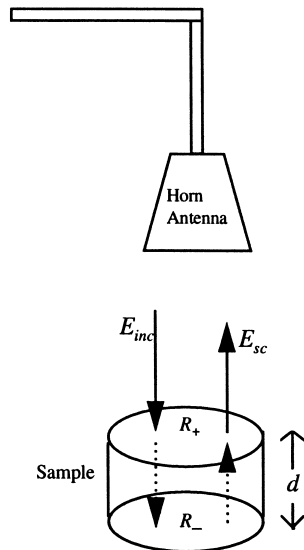


Fig. 1. Experimental set-up to measure the dielectric properties of materials using a step frequency radar. The radar ‘steps’ through many frequencies, and measures the steady state response (magnitude and phase) from the sample at each frequency.

At present, there are a number of direct methods (see the survey in [15]) for measuring the electrical properties of ice. One method, described in [13], involves a probe that is inserted into ice in situ. There is concern, however, that measurements done in this way may be affected in an unknown way by boundary effects on the surface of the probe and by ice at some distance from the probe.

A second method, developed in [17] and used in [9–11,15], generally requires removal of an ice core. In particular, the procedure used by Lytle and Ackley [11] involves cutting an ice core into short sections about 6 cm long, milling the cut ends to be very flat and parallel, and placing the ice on a styrofoam platform in a cold room held at a constant temperature (Fig. 1). They then direct a stepped-frequency radar (discussed below) at the ice. The measured data is used to synthesize the response of the medium to a short (0.1 ns) pulse. The time-domain plot of the reflected pulse shows two peaks, one from the top surface of the ice and one from the bottom. They assume that the electrical properties of the ice are constant throughout the sample, which enables them to obtain the electrical permittivity from the time between the peaks, and the electrical conductivity from the relative magnitudes of the peaks.

This method meets with some difficulty for ice samples that are relatively warm. At higher temperatures, a larger fraction of the sample is composed of brine, which tends to drain out when the ice core is removed for study. Moreover, the large brine fraction makes the ice highly conductive, which causes the second peak, from the ice bottom, to be so small as to be indistinguishable from noise. This second peak can be made larger by making the sample thinner, which is mechanically difficult, and reduces the accuracy of the results. For samples with a high brine volume (greater than about 5%), it is not possible to use this method to extract the electrical properties.

Because of the questions and difficulties with these available methods, there is interest in development of the other methods for obtaining the electrical properties of ice, particularly remote methods that would not require removal and handling of ice cores and which could measure the

electrical parameters of ice with a high brine volume. One such method is to find the medium parameters directly from the surface reflection.

Another reason to develop a method for finding medium parameters from surface reflections is that this is a key step in some methods for reconstructing the interior electrical properties. In theory, measurements of a complete set of radar reflections probably suffices to determine the entire spatial distribution of electrical parameters in the medium (see the related work, [12,14]). One way of trying to reconstruct this distribution is to use a layer-stripping algorithm [3,16,18,19], in which one first finds the electrical parameters on the surface, and then mathematically strips away the top surface and synthesizes measurements that would have been obtained if the top surface had been absent. The process is repeated, and the medium is mathematically stripped away, layer-by-layer, with the electrical parameters being found in the process.

The first step in such a layer-stripping algorithm is to find the electrical parameters on the surface, and it is this problem that we consider in this paper. The method presented is based on the idea that the first return pulse must contain information about the surface. This idea applies not only to ice and electromagnetic waves, but also to any wave propagation problem, and the formulas in this paper apply to any problem governed by Eq. (2.9) below.

This method presented here is closely related to a method pioneered by Kralj and Carin [7], who used the reflection of a short pulse from an interface to determine the electrical parameters of water. Their method is somewhat different from the one described below in that they reduce the problem to a homogenous half-space. The method below is described for data obtained from a stepped-frequency radar.

2. Background

The propagation of electromagnetic waves is governed by Maxwell’s equations, which we write in the form:

$$\nabla \wedge \mathcal{E} = -\frac{\partial \mu \mathcal{H}}{\partial t} \tag{2.1}$$

$$\nabla \wedge \mathcal{H} = \sigma \mathcal{E} + \frac{\partial \epsilon \mathcal{E}}{\partial t}. \tag{2.2}$$

Here $\mathcal{E} = (\mathcal{E}_x, \mathcal{E}_y, \mathcal{E}_z)$ is the electric field, $\mathcal{H} = (\mathcal{H}_x, \mathcal{H}_y, \mathcal{H}_z)$ the magnetic field, ϵ the electric permittivity, μ the magnetic permeability, and σ the conductivity.

The magnetic permeability of sea ice, air, and water is very close to the permeability of free space; accordingly we assume $\mu = \mu_0$. If we write out the six scalar equations, Eqs. (2.1) and (2.2), and assume that ϵ , σ , \mathcal{E} , and \mathcal{H} are independent of one of the coordinates, say y , then we find that six equations decouple into two sets of equations, one set for \mathcal{H}_x , \mathcal{E}_y , and \mathcal{H}_z , and the other set for \mathcal{E}_x , \mathcal{H}_y , and \mathcal{E}_z . These determine independent polarizations, the former called the Transverse Electric (TE) polarization and the the latter called the Transverse Magnetic (TM) polarization [5].

The equations for the TE polarization reduce to:

$$\nabla^2 \mathcal{E} - \mu_0 \epsilon \frac{\partial^2 \mathcal{E}}{\partial t^2} - \mu_0 \sigma \frac{\partial \mathcal{E}}{\partial t} = 0, \tag{2.3}$$

where the Laplacian is a two-dimensional one in the x and z variables, and we have dropped the subscript y . We assume that the upper half-space ($z > 0$) is air, which we approximate by the same electromagnetic parameters as free space, namely $\epsilon = \epsilon_0$, $\sigma = 0$. The permittivity and conductivity of the lower half-space are allowed to vary in any manner with x and z . This possible spatial dependence of the lower half-space is immaterial, because we will consider only the initial reflection from the surface.

Experiments are carried out as follows. The horn antenna emits a single-frequency downgoing wave that, near the axis of the antenna, is of the form $\cos(i\omega(t + z/c_0)) = \text{Re } e^{-i\omega(t+z/c_0)}$, where $c_0 = 1/\sqrt{\mu_0\epsilon_0}$ is the speed of light in the air. The corresponding solution to Eq. (2.3) is $\mathcal{E} = \text{Re } e^{-i\omega t} E$, where E satisfies:

$$(\nabla^2 + \omega^2\mu_0\epsilon + i\omega\mu_0\sigma)E = 0. \quad (2.4)$$

Within the antenna horn, the field is a superposition of downgoing and upgoing waves:

$$e^{-i\omega t} E(\omega, z) = e^{-i\omega(t+z/c_0)} + R(\omega)e^{-i\omega(t-z/c_0)}, \quad (2.5)$$

where R denotes the reflection coefficient. We will use the notation $E = E_{\text{inc}} + E_{\text{sc}}$, where $E_{\text{inc}}(\omega, z) = \exp(-i\omega z/c_0)$ and $E_{\text{sc}}(\omega, z) = R(\omega)\exp(i\omega z/c_0)$.

This form for the incident wave is not a good global model for the wave emanating from a real antenna, and this form for the scattered wave is not generally valid in the case of a lower half-space with lateral variations. However, the antenna sidelobes and the lateral variation of the lower half-space will cause disturbances that arrive back at the antenna at a time later than that of the first reflection. Because we consider only the initial arrival of the scattered wave, we use a simple one-dimensional model.

The stepped-frequency radar first emits one frequency and measures the steady-state response, both in magnitude and phase, and then it steps up to another frequency and repeats the process. It does this for a large number of frequencies in some band. For example, the Lytle–Ackley work [11] uses 801 frequencies equally spaced between 26.5 and 40 GHz.

These frequency-domain measurements can be used to synthesize the response to an incident pulse in the time domain. If we knew E at all frequencies, to get the impulse response, we would use the Fourier transform:

$$\mathcal{E}^\infty(t, z) = \int E(\omega, z)e^{-i\omega t} d\omega. \quad (2.6)$$

We will use the notation defined below Eq. (2.5) in the time domain as well, so that $\mathcal{E}^\infty = \mathcal{E}_{\text{inc}}^\infty + \mathcal{E}_{\text{sc}}^\infty$, where $\mathcal{E}_{\text{inc}}^\infty(t, z) = \delta(t + z/c_0)$ and $\mathcal{E}_{\text{sc}}^\infty(t, z) = \mathcal{R}^\infty(t - z/c_0)$. Here \mathcal{R}^∞ is the Fourier transform of R .

For the case of stepped-frequency radar, we use a band-limited approximation to Eq. (2.6) namely:

$$\mathcal{E}(t, z) = \sum_j E(\omega_j, z)w_j e^{-i\omega_j t}, \quad (2.7)$$

where the w_j are weights chosen to minimize ringing due to Gibb's phenomenon. These issues will be discussed more fully in Section 3.

In order to obtain information about the first return pulse, we use a short-time expansion called the progressing wave expansion [4,8]. If the incident wave is the downgoing, normal-incidence, delta

function plane wave $\delta(t + z/c_0)$, then the corresponding upgoing scattered wave \mathcal{E}_{sc}^∞ can be expanded in the form:

$$\mathcal{E}_{sc}^\infty(t, z) = \tilde{A}_0\delta(t - z/c_0) + \tilde{A}_1H(t - z/c_0) + \dots, \tag{2.8}$$

where H denotes the Heaviside function that is one for positive arguments and zero for negative arguments. In this expansion, each term is proportional to the derivative of the following term. The remainder terms, denoted by dots, are continuous and zero at the origin.

Expansion Eq. (2.8) is problematic because t and z/c_0 still carry the units of time. Because of this, the ratios of successive terms in the sequence $\tilde{A}_0, \tilde{A}_1, \dots$ involve a factor of c_0 , the speed of light, which is roughly 3×10^8 m/s.

To get rid of the dimensions, we will write $k = \omega L/c_0$, where $c_0 = (\mu_0\epsilon_0)^{-1/2}$ is the speed of light in free space and L is an arbitrary constant with the dimensions of length. We will consider only k positive. In addition, we write $n^2 = \epsilon/\epsilon_0$ and $m = \sigma\sqrt{\mu_0/\epsilon_0}$. With this notation, Eq. (2.4) becomes:

$$\left(\nabla^2 + k^2\frac{n^2}{L^2} + ik\frac{m}{L}\right)E = 0, \tag{2.9}$$

where we have dropped the subscript on E . Both n^2 and m are assumed nonnegative. We assume that n^2 is identically one and m is identically zero in the upper half-space. The parameter values of sea ice in the gigahertz range are between 3 and 4 for n^2 and around 6 m^{-1} for m . For sea water, n^2 is 3.37, and the value of m is around 7000 m^{-1} [2].

With the change of variables $k = \omega L/c_0$, Eq. (2.5) becomes:

$$e^{-ik\tau}E(k, z) = e^{-ik(\tau+z)} + R(k)e^{-ik(\tau-z)} \tag{2.10}$$

and Eq. (2.6) becomes:

$$\mathcal{E}^\infty(\tau, z) = \frac{c_0}{L} \int E(k, z)e^{ik\tau} dk \tag{2.11}$$

where $\tau = c_0t/L$. Expansion Eq. (2.8) becomes:

$$\mathcal{E}_{sc}^\infty(\tau, z) = \mathcal{R}(\tau - z) = A_0\delta(\tau - z) + A_1H(\tau - z) + \dots \tag{2.12}$$

Standard methods of geometrical optics [8] can be used to find the coefficients A_0 and A_1 ; they turn out to be:

$$A_0 = \frac{1 - n}{1 + n} \tag{2.13}$$

and

$$A_1 = \frac{(m + \partial_z n)L}{n(1 + n)^2}. \tag{2.14}$$

If the medium varies with depth, Eq. (2.14) does not allow us to separate m from $\partial_z n$. In this case, two different angles of incidence can be used, and a different formula, given in [3], can be used to find both

m and $\partial_z n$. Here, for simplicity, we will assume that the medium does not vary with depth near the surface, so that knowledge of A_0 and A_1 enables us to recover both n and m and hence the permittivity and conductivity.

The method of Kralj and Carin [7] assumes that \mathcal{E}_{sc}^∞ is the reflection from a homogeneous half-space. They then Fourier transform into the frequency domain and use Eqs. (4.1) and (4.2), below, to recover the desired parameters. Their method has the advantage of not making any assumption about the dispersion of the medium; however, it is difficult to see how to extend their method to the case in which the medium varies with depth.

The time-domain expansion Eq. (2.12) is closely related to the frequency-domain expansion:

$$R(k) = a_0 + \frac{a_1}{ik} + \dots \tag{2.15}$$

The expansion coefficients $1, (ik)^{-1}$ of Eq. (2.15) are related to the δ, H, \dots of Eq. (2.12) by the Fourier transform:

$$\delta(\tau) = \int 1e^{-ik\tau} dk, H(\tau) = \text{P.V.} \int \frac{e^{-ik\tau}}{ik} dk, \dots, \tag{2.16}$$

where ‘P.V.’ denotes principal value.

Each term in the frequency-domain expansion Eq. (2.15), however, can contain components with different phases. For example, the order-one term a_0 can be written:

$$a_0 = A_0 + B_0 e^{ikb_0} + \dots \tag{2.17}$$

Here A_0 corresponds to the first return, as in Eq. (2.12), and the higher terms correspond to arrivals at later times. It is A_0 that contains only information about the surface; the other terms contain information about propagation through other parts of the medium. It is to separate out this first return that we must use the time-domain expansion Eq. (2.12).

3. The band-limited geometrical optics method

In dealing with data from a stepped-frequency radar, we cannot use Eqs. (2.10) and (2.16) directly, because we have measurements from only a finite number of frequencies k_0, k_1, \dots, k_N . Accordingly, instead of integrals, we use finite sums. The scaled version of Eq. (2.7) is:

$$\mathcal{R}(\tau) = \sum_j R(k_j) w_j e^{-ik_j \tau}. \tag{3.1}$$

We assume that $k_j = k_0 + j(B/N)$, where B denotes the frequency bandwidth. Consequently, each term of Eq. (3.1) contains a factor $e^{-ik_0 \tau}$, which we factor out. We write the quotient as:

$$f(\tau) = e^{ik_0 \tau} \mathcal{R}(\tau) = \sum_j R(k_j) w_j e^{-ij\tau B/N}. \tag{3.2}$$

In place of Eq. (2.16), we will use:

$$p(\tau) = \sum_j w_j e^{-ij\tau B/N}, \quad h(\tau) = \sum_j \frac{w_j}{ik_j} e^{-ij\tau B/N}, \dots \tag{3.3}$$

The weights w_j , used to minimize ringing due to Gibbs’ phenomenon, can be chosen to be, say, Hamming weights. We note that Eqs. (3.2) and (3.3) are periodic in τ , with period $2\pi N/B$.

From Eqs. (2.15), (2.17), (3.2) and (3.3), we obtain:

$$f(\tau) = A_0 p(\tau) + A_1 h(\tau) + r(\tau), \tag{3.4}$$

where r denotes a remainder term that is continuous and zero at the origin. The left side of Eq. (3.4) is known from measurements; from it we want to extract A_0 and A_1 .

To do this, we minimize the least-squares error:

$$\int_0^T |f(\tau) - A_0 p(\tau) + A_1 h(\tau) - r(\tau)|^2 d\tau. \tag{3.5}$$

Differentiating with respect to A_0 and A_1 leads to the system of equations:

$$MA + Q = F, \tag{3.6}$$

where $A = (A_0, A_1)^t$:

$$F = \left(\operatorname{Re} \int_0^T f(\tau) \overline{p(\tau)} d\tau, \operatorname{Re} \int_0^T f(\tau) \overline{h(\tau)} d\tau \right)^t, \tag{3.7}$$

where the bar denotes complex conjugate and the superscript t denotes transpose, where M is the matrix with entries:

$$M_{11} = \int_0^T |p(\tau)|^2 d\tau, \tag{3.8}$$

$$M_{22} = \int_0^T |h(\tau)|^2 d\tau, \tag{3.9}$$

$$M_{12} = M_{21} = \operatorname{Re} \int_0^T h(\tau) \overline{p(\tau)} d\tau, \tag{3.10}$$

and where:

$$Q = \left(\operatorname{Re} \int_0^T \overline{p(\tau)} r(\tau) d\tau, \operatorname{Re} \int_0^T \overline{h(\tau)} r(\tau) d\tau \right)^t. \tag{3.11}$$

In what follows, we assume that T is so small that Q is negligible.

We substitute Eq. (3.3) into Eqs. (3.7)–(3.10) and carry out the τ integration. The τ integration results in the quantity y_j , which is defined as:

$$y_j = \int_0^T e^{ij\tau B/N} d\tau = \begin{cases} T & \text{if } j = 0 \\ \frac{e^{ijTB/N} - 1}{ijB/N} & \text{if } j \neq 0. \end{cases} \quad (3.12)$$

With this notation, Eqs. (3.7)–(3.10) becomes:

$$F = \left(\operatorname{Re} \sum_{n,m=0}^N w_n w_m R_m y_{n-m}, \operatorname{Re} \sum_{n,m=0}^N w_n \frac{w_m}{ik_n} R_m y_{n-m} \right)^t \quad (3.13)$$

$$M_{11} = \sum_{n,m=0}^N w_n w_m y_{n-m} \quad (3.14)$$

$$M_{22} = \sum_{n,m=0}^N \frac{w_n w_m}{k_n k_m} y_{n-m} \quad (3.15)$$

$$M_{12} = M_{21} = \operatorname{Re} \sum_{n,m=0}^N w_n \frac{w_m}{ik_m} y_{n-m}. \quad (3.16)$$

In summary, the method to reconstruct the surface parameters is as follows. Measure the reflection coefficient $R_j, j = 0, \dots, N$ for the available (equally-spaced) frequencies. Use Eqs. (3.13) and (3.12) to construct F . Solve the equation $MA = F$, where M is given by Eqs. (3.14)–(3.16), to obtain $A = (A_0, A_1)$. Solve Eq. (2.13) for n , and solve Eq. (2.14) for m , assuming that $\partial_z n = 0$.

4. Performance of the method

To determine the possible utility of the band-limited geometrical optics method, we have tested it on synthetic data. To generate the data, we used the following well-known formula [6] for the reflection coefficient from a two-layer medium. We denote the electrical parameters of the upper half-space by $n_+ = 1$ and $m_+ = 0$, the parameters of the intermediate layer by n and m , and the parameters of the lower half-space by n_- and m_- . We assume that the intermediate layer has thickness d . The reflection coefficient at the top interface is:

$$R_+ = \frac{1 - \eta_+}{1 + \eta_+}, \quad (4.1)$$

where

$$\eta_+ = \sqrt{n^2 + \frac{im}{k}} \quad (4.2)$$

the reflection coefficient at the bottom interface is:

$$R_- = \frac{1 - \eta_-}{1 + \eta_-}, \quad (4.3)$$

Table 1
Reconstructions from simulated noisy data

Thickness	Noise amp.	n^2 mean	n^2 st. dev.	σ mean	σ st. dev.
Frequency band 26.5 to 40 GHz (skin depth ≈ 0.03 m)					
0.1	0.001	3.3700	0.003	0.0170	0.0007
0.1	0.01	3.3688	0.034	0.0178	0.0081
0.1	0.1	3.3732	0.033	0.0211	0.0592
0.05	0.001	3.3665	0.0035	0.0167	0.0008
0.05	0.01	3.3594	0.0299	0.0157	0.0085
0.05	0.1	3.4843	0.0365	0.0008	0.0862
Frequency band 1 to 4 GHz (skin depth ≈ 0.15 m)					
0.1	0.001	3.4100	0.0013	0.0182	0.0001
0.1	0.01	3.4131	0.0132	0.0181	0.0006
0.1	0.1	3.3854	0.1288	0.0171	0.0051
0.5	0.001	0.6224	0.0002	-0.0709	0.00003
0.5	0.01	0.6226	0.0018	-0.0709	0.0002
0.5	0.1	0.4406	0.2122	-0.0284	0.0500

where

$$\eta_- = \sqrt{\frac{n_-^2 + im_-/k}{n^2 + im/k}} \tag{4.4}$$

With this notation, the two-layer reflection coefficient is:

$$R = \frac{R_+ + R_- e^{2ik\eta_+ d}}{1 + R_+ R_- e^{2ik\eta_+ d}} \tag{4.5}$$

After computing the two-layer reflection coefficient, we added random noise, with magnitude α , to the real and imaginary parts. We then used the band-limited geometrical optics method above to reconstruct n^2 and σ .

In each case, we used the same values of n^2 and m to compute the data, namely $n^2 = 3.37$ and $\sigma = 0.017$. We considered two different frequency bands, namely 1 to 4 GHz and 26.5 to 40 GHz. Because the longer wavelength waves penetrate deeper into the medium, we also considered media of different thickness. We chose the T in Eqs. (3.5) and (3.12) to be $\pi/(2B)$.

The results are shown in Table 1. In each case, the means and standard deviations are calculated from 35 samples. The Appendix shows how we arrived at the number 35. All units are standard MKS units.

We have also made some preliminary tests of this method on experimental data. The data was collected as described in Section 1, using an HP8510 network analyzer configured as a step frequency radar. The data was composed of $\tilde{N} = 801$ measurements of the reflection coefficient, for equally spaced frequencies between 26.5 and 40 GHz. To use this data, we first did some processing to isolate and calibrate the response from the top surface. In particular, we performed the following operations.

1. We transformed into the time domain, using an FFT padded out to length $32\tilde{N}$ with zeros. We shifted the main peak to time zero, and transformed back into the frequency domain.
2. We multiplied by a Hamming window (`hamming(801)` in Matlab), transformed into the time domain with an FFT padded to length $4\tilde{N}$. In the time domain we multiplied by a gating function (`hamming(11)` in Matlab). This isolates the reflection from the top surface. Finally, we transformed back to the frequency domain and multiplied by a correction to remove the effects of the windowing and gating.
3. We performed the same operations to data obtained from an aluminum reflector. Because the reflection coefficient from an aluminum sheet should be -1 , this gives us a correction factor that accounts for the system response.
4. We used this correction factor to multiply the ice data, which had been already processed by steps 1 and 2.

This procedure, followed by the band-limited geometrical optics method, gave us a value of $n^2 = 2.42$ for a lucite sample, versus $n^2 = 2.48$ as computed by the ‘bounce’ method of [15] and [11]. The method did not return a reasonable value for m .

The method did not give reasonable values on the ice datasets.

There are many possible reasons for our lack of success with real data. First, the mathematical model Eq. (2.3) may not be adequate. It is based on the questionable assumption that ϵ and σ are frequency-independent. Moreover, our recovery of m from Eq. (2.14) is based on the assumption that the permittivity does not change with depth. Although this is probably true for lucite, it is unlikely to be true for the ice samples. To avoid making this assumption, we would need bistatic measurements for at least one more angle of incidence.

A second possible reason for the poor performance of the method is that the real data is affected by many factors not included in the model described here. Although time gating and normalizing to a known reflector make the data appear considerably cleaner, this process also introduces errors. Moreover, there may be unmodelled effects due to beam spreading, reflection from the sides of the ice core, and scattering from the brine pockets.

A third possible reason for the poor performance is that the experimental errors may be too large. Although the electronic instrumentation is quite stable, and repeated measurements give the same results out to the third decimal place, realignment of the sample could cause changes in the measurements as large as 10%. This method is likely to be more sensitive to errors than the more robust transmission method [11,15], because the transmission method compares two different reflected pulses arising from the same incident pulse. Small misalignments therefore may cancel each other out, to some degree, when the two pulses are compared. The present method, however, compares the surface reflected pulse with a theoretical ideal, and is therefore more subject to experimental errors such as those due to misalignments.

5. Conclusions and suggestions for further work

The simulation studies suggest that the band-limited geometrical optics method may be useful for finding the surface conductivity and permittivity from normal-incidence radar reflections.

Further development of this method would involve consideration of a variety of effects. In particular, from the bottom three lines of Table 1, it is evident that when the method is applied to a non-uniform medium, the result is not simply an average of the medium parameters over some small region. It would be useful to understand this phenomenon.

Acknowledgements

The work of MC and DI was supported in part by the Office of Naval Research grant N00014-93-1-0048. MC’s work was also supported by the National Science Foundation Faculty Award for Women in Science and Engineering, DMS 9023630, by Rensselaer Polytechnic Institute, and by the Minnesota Institute for Mathematics and its Applications. She is grateful to Prasad Gogineni for teaching her how to remove the system response from the data, and to Bob Onstott for many helpful conversations.

The work of VL and SA was supported in part by Office of Naval Research grant number N0001495MP30019.

Appendix

A. How many samples are needed?

In this appendix, we estimate the number of samples needed to ensure that the average is sufficiently close to the statistical mean. By ‘sufficiently close’, we mean that the two quantities are within a given tolerance β of each other. We denote our individual measurements by s_j , $j = 1, 2, \dots, J$. These measurements are samples of a random variable s , which for simplicity we assume to have means $\langle s \rangle = 0$. We want to find J so that the mean-square deviation between the average and the mean is less than β , i.e.:

$$\sqrt{\left\langle \left(\frac{1}{J} \sum_{j=1}^J s_j - \langle s \rangle \right)^2 \right\rangle} < \beta. \tag{A.1}$$

Because the mean $\langle s \rangle$ is zero and the samples are assumed to be identically distributed and independent, Eq. (A.1) simplifies to:

$$\frac{1}{\sqrt{J}} \sqrt{\langle s^2 \rangle} < \beta. \tag{A.2}$$

We assume that s is uniformly distributed between $-\alpha$ and α , so that we can compute the expected value of s^2 as:

$$\langle s^2 \rangle = \frac{1}{2\alpha} \int_{-\alpha}^{\alpha} s^2 ds = \frac{\alpha^2}{3}. \tag{A.3}$$

Inequality Eq. (A.2) thus becomes:

$$\frac{1}{\sqrt{J}} \sqrt{\frac{\alpha^2}{3}} < \beta, \quad (\text{A.4})$$

which we can solve for J to obtain:

$$J > \frac{\alpha^2}{3\beta^2}. \quad (\text{A.5})$$

Thus to obtain an approximation to $\langle s \rangle$ that is good to three decimal places ($\beta = 10^{-3}$), if the noise amplitude is $\alpha = 10^{-2}$, we should take at least 34 samples, and if the noise amplitude is $\alpha = 10^{-3}$, we need to take only one sample.

These calculations apply when we know the statistics of the samples. However, in our case, we know the statistics of the measurements of the reflection coefficients, and then we compute the ice parameters by a complicated nonlinear process, and what we wish to know is the statistics of the results. These calculations, therefore, merely serve as general guidelines.

References

- [1] S.F. Ackley, *Sea Ice*, *Encycl. of Appl. Physics*, vol. 17, VCH Publishers, 1996.
- [2] F.D. Carsey (Ed.), *Microwaves Remote Sensing of Sea Ice*, *Geophysical Monograph* 68, American Geophysical Union, 1992.
- [3] M. Cheney, D. Isaacson, Inverse problems for a perturbed dissipative half-space, *Inverse Problems* 11 (1995) 865–888.
- [4] R. Courant, D. Hilbert, *Methods of Mathematical Physics*, vol. 2, Wiley, New York, 1962.
- [5] J.D. Jackson, *Classical Electrodynamics*, 2nd ed., Wiley, New York, 1975.
- [6] J.A. Kong, *Electromagnetic Wave Theory*, 2nd ed., Wiley, New York, 1990.
- [7] D. Kralj, L. Carin, Ultra-wideband characterization of lossy materials: short-pulse microwave measurements, *IEEE MTT-S International Microwave Symposium Digest* 3 (1993) 1239–1242.
- [8] M. Kline, I. Kay, *Electromagnetic Theory and Geometrical Optics*, Wiley, New York, 1965.
- [9] G. Koh, Dielectric constant of ice at 26.5–40 GHz, *J. Appl. Phys.* 71 (1992) 5119–5122.
- [10] G. Koh, Experimental study of electromagnetic wave propagation in dense random media, *Waves in Random Media* 2 (1992) 39–48.
- [11] V.I. Lytle, S.F. Ackley, Permittivity of sea ice at Ka-Band, *Proc. IGARRS'95*, Florence, Italy, July 1995, pp. 410–413.
- [12] M. Lassas, M. Cheney, G. Uhlmann, Uniqueness for a wave propagation inverse problem in a half-space, *Inverse Problems* 14 (1998) 679–684.
- [13] E. Nassar, R. Lee, K. Jezek, J. Young, 1996. In situ measurements of the complex dielectric constant of sea ice from 1 to 10 GHz, *Proceedings, IGARSS'96*, pp. 118–120.
- [14] P. Ola, L. Päiväranta, E. Somersalo, An inverse boundary value problem in electrodynamics, *Duke Math. J.* 70 (1993) 617–653.
- [15] R.L. Rennie, Dielectric measurements of sea ice in the frequency range 26.5 to 40 GHz using a quasi-optical technique, Master's thesis, Dartmouth College, Hanover, NH, 1991.
- [16] J. Sylvester, Layer stripping for the Helmholtz equation, *SIAM J. Appl. Math.* 56 (1996) 736–754.
- [17] A. Stogryn, G.J. Desargant, The dielectric properties of brine in sea ice at microwave frequencies, *IEEE Trans. Antennas Propagation* AP-33 (1985) 523–531.

- [18] E. Somersalo, Layer-stripping for time-harmonic Maxwell's equations with fixed frequency, *Inverse Problems* 10 (1994) 449–466.
- [19] E. Somersalo, M. Cheney, D. Isaacson, E. Isaacson, Layer stripping: a direct numerical method for impedance imaging, *Inverse Problems* 7 (1991) 899–926. Erratum; *Inverse Problems* 8 (1992) 493.
- [20] W.F. Weeks, S.F. Ackley, in: N. Untersteiner (Ed.), *Structure and Properties of Sea Ice, Geophysics of Sea Ice*, NATO ASI Series, Physics, vol. 146, Plenum Press, New York, Chap. 1, 1986.